

Supplementary Information

Blocking and bridging ligands direct the structure and magnetic properties of dimers of pentacoordinate nickel(II)

*Luisa López-Banet,^a M. Dolores Santana,^a * Gabriel García,^a José Pérez,^b Luís García,^b Luis Lezama^c and Ivan da Silva^d*

^a Departamento de Química Inorgánica and Regional Campus of International Excellence (Campus Mare Nostrum), Universidad de Murcia, E-30071 Murcia, Spain.

^b Departamento de Ingeniería Minera, Geológica y Cartográfica. Área de Química Inorgánica, Universidad Politécnica de Cartagena, E-30203 Cartagena, Spain.

^c Departamento de Química Inorgánica, Facultad de Ciencia y Tecnología, Universidad del País Vasco UPV/EHU, P.O. Box 644, 48080 Bilbao, Spain. BCMaterials, Parque Científico y Tecnológico de Bizkaia, Edificio 500-1, 48160 Derio, Spain.

^d ISIS Facility, Rutherford Appleton Laboratory, Chilton, Oxfordshire, OX11 0QX UK

Table S1. Crystallographic data for complexes **1** – **5**.

Complex	1	2	3	4.CH₂Cl₂	5
Formula				C45 H54 B2 Cl4 Ni4 Ni2 O2	C26 H50 F12 N6 Ni2 O4 P2
<u>M</u>				1103.86	918.08
Crystal system	orthorhombic	orthorhombic	orthorhombic	monoclinic	monoclinic
Space group	Pnmm	Pnmm	Pnmm	C2/c	P21/n
<u>Z</u>				4	2
<i>a</i> / Å	17.1572(2)	17.24479(18)	17.3543(2)	17.9483(17)	8.1736(4)
<i>b</i> / Å	13.65435(14)	13.66574(12)	13.69393(14)	19.1658(18)	15.1274(8)
<i>c</i> / Å	7.88214(7)	7.88513(6)	7.89244(8)	15.6504(15)	14.9948(8)
α / °	90	90	90	90	90
β / °	90	90	90	103.780(2)	90.6130(10)
γ / °	90	90	90	90	90
<i>V</i> / Å ³	1846.55(3)	1858.23(3)	1875.63(4)	5228.7(9)	1853.93(17)
<i>T</i> / K				100(2)	100(2)
λ / Å	0.82449	0.82449	0.82449	0.71073	0.71073
μ / mm ⁻¹				1.402	1.203
Reflections collected				6409	4329
Independent reflections				5622 (326)	4026 (235)
Goodness-of-fit on <i>F</i> ²				1.085	1.243
Final <i>R</i> indices				0.0865	0.0588
[<i>I</i> > 2σ(<i>I</i>)] ^[a,b]				0.0946	0.0646
<i>R</i> indices (all data) ^[a,b]				0.2423	0.1243
Max /min				5.220	0.641
$\Delta\rho$ [e · Å ⁻³]				-1.185	-0.506

^[a] $R_1 = \sum \left| |F_o| - |F_c| \right| / \sum |F_o|$ for reflections with $I > 2\sigma I$. ^[b] $wR_2 = \left\{ \frac{\sum [w(F_o^2 - F_c^2)^2]}{\sum [w(F_o^2)]} \right\}^{1/2}$ for all reflections;

$w^{-1} = \sigma^2(F^2) + (aP)^2 + bP$, in which $P = (2F_c^2 + F_o^2)/3$ and a and b are constants set by the program.

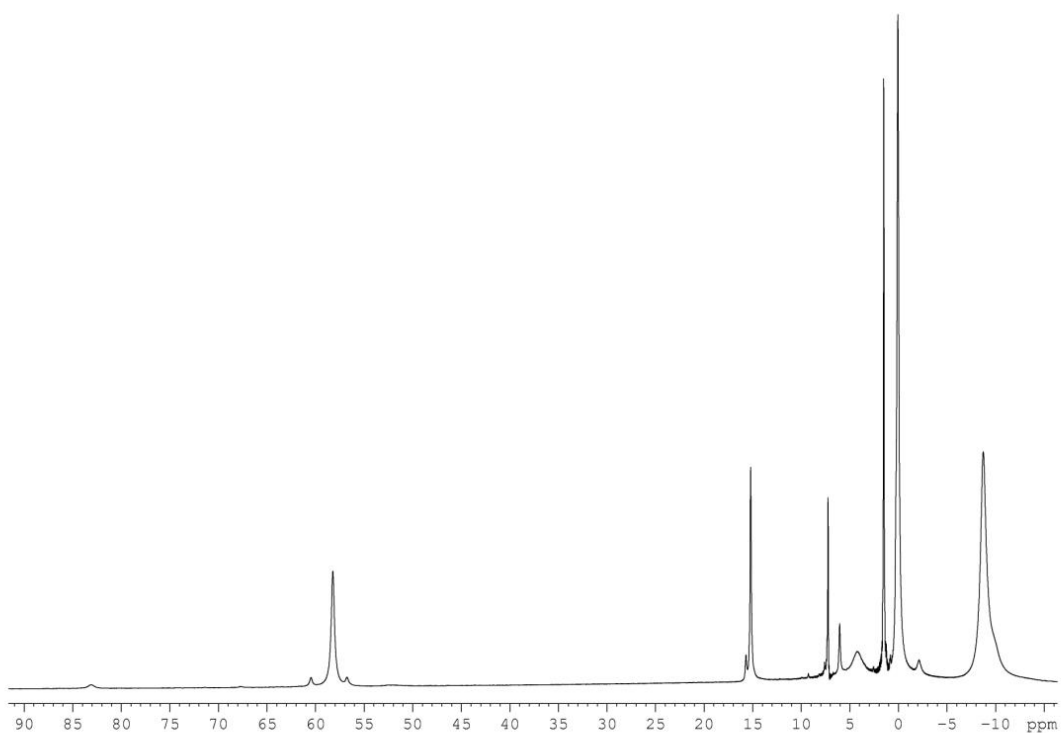


Figure S1. ^1H NMR spectrum of **4** in CDCl_3 solution at r.t.

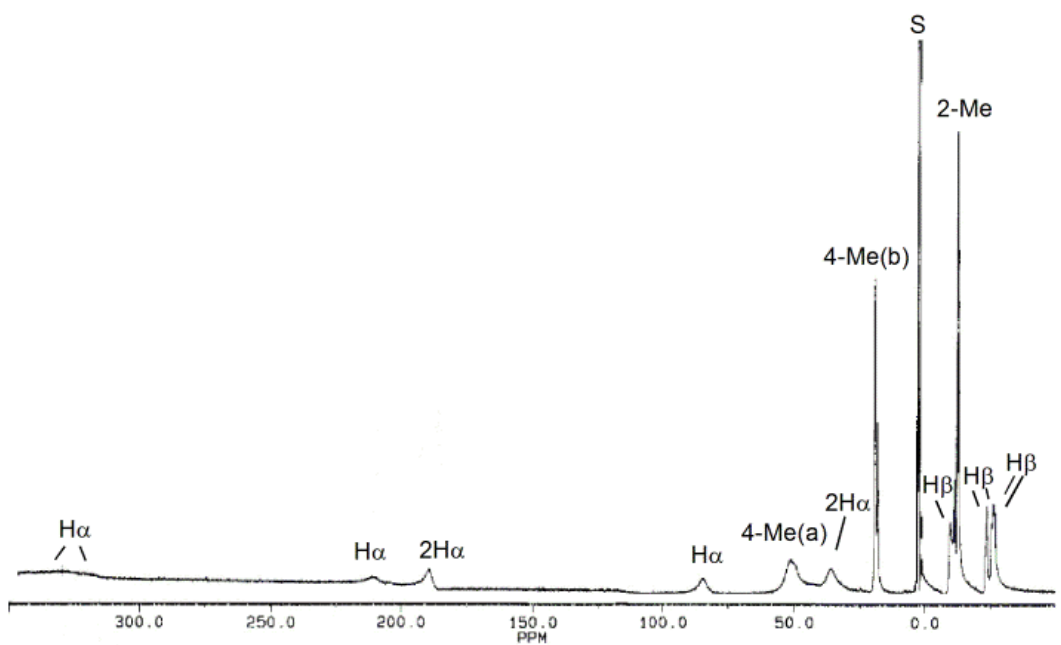


Figure S2. ^1H NMR spectrum of **5** in $(\text{CD}_3)_2\text{CO}$ solution at r.t.

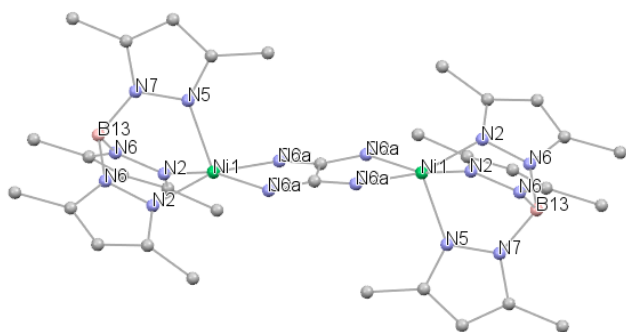


Figure S3. Drawing of complex **2** with the atomic numbering around Ni(II) ions.

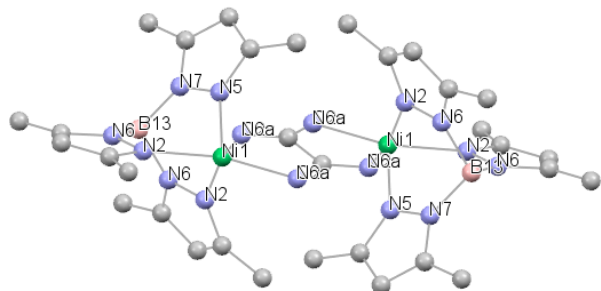


Figure S4. Drawing of complex **3** with the atomic numbering around Ni(II) ions.

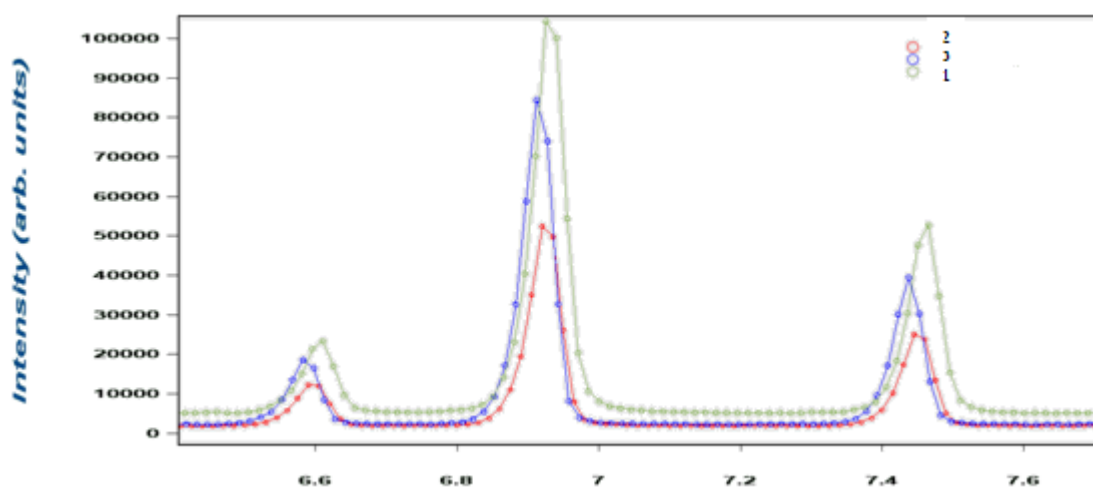


Figure S5. Selected low angle diffractograms of complexes **1** – **3**.

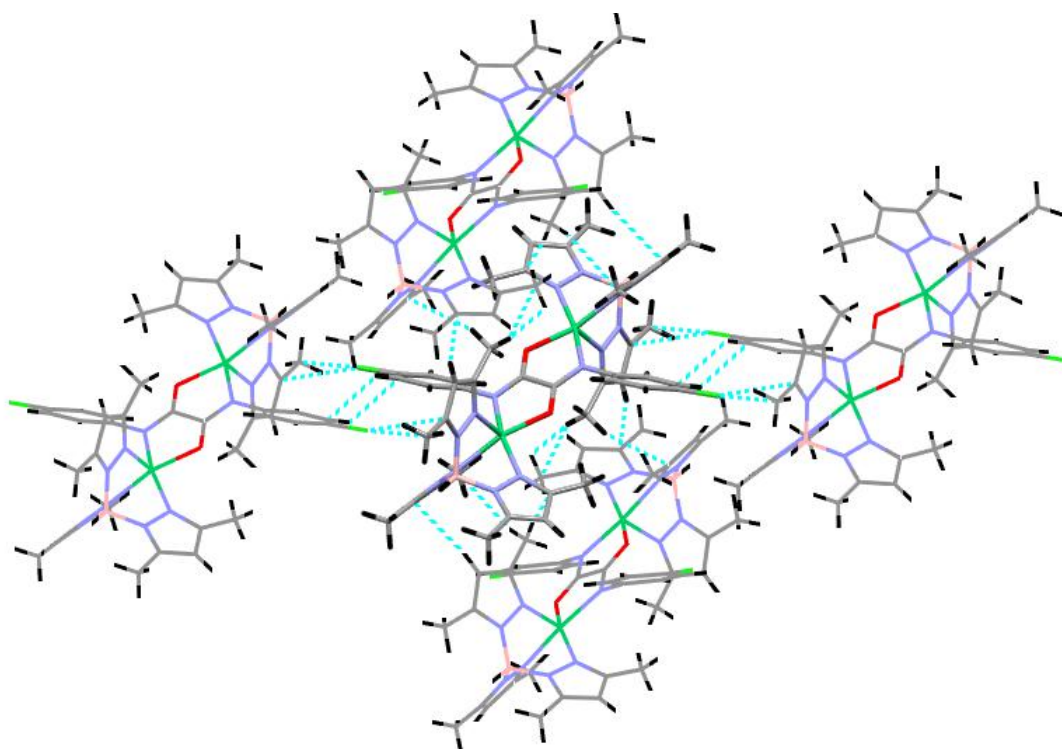


Figure S6. Molecular packing of complex 4 showing CH \cdots π interactions.

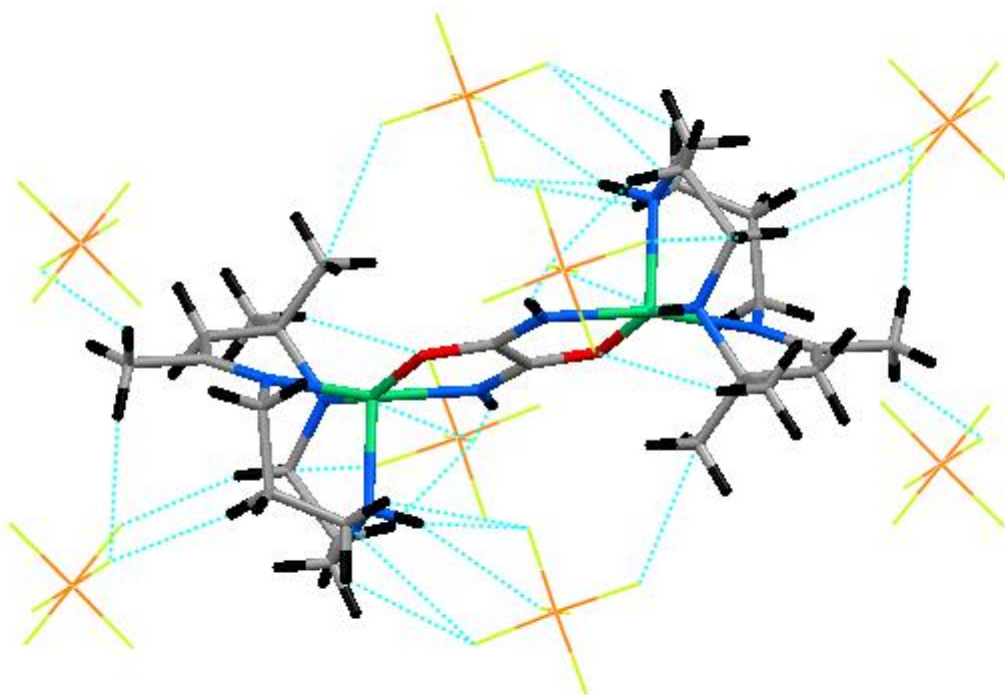


Figure S7. Molecular packing of $\{[\text{Ni}(\text{N}_3\text{-mc})_2(\mu\text{-oa})]\text{(PF}_6)_2\}$ showing supramolecular interactions.

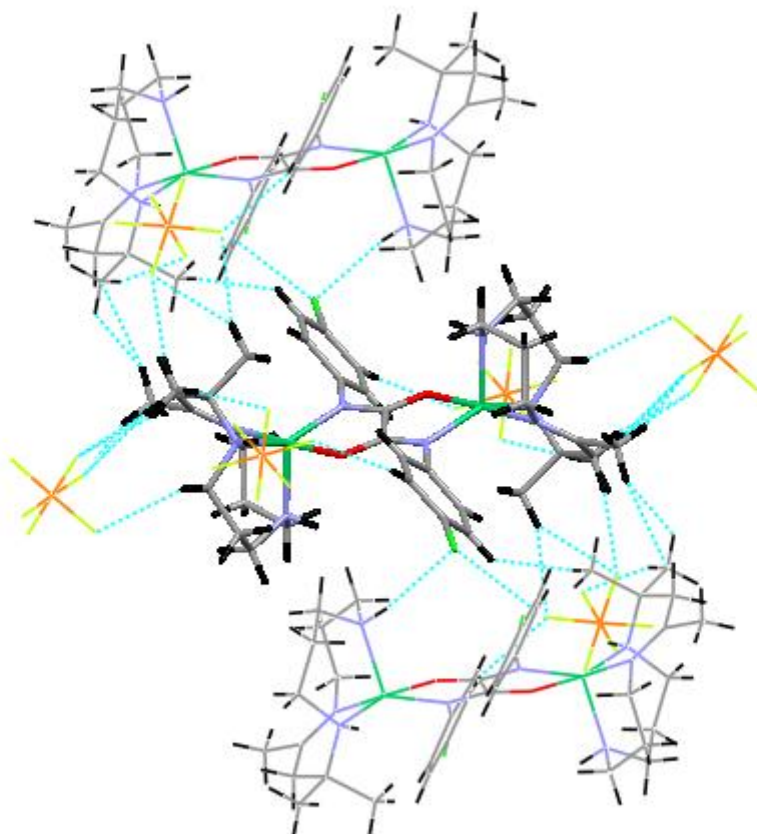


Figure S8. Molecular packing of $\{[\text{Ni}(\text{N}_3\text{-mc})]_2[\mu\text{-CO}(4\text{-Cl-C}_6\text{H}_4\text{-N})]_2\}(\text{PF}_6)_2$ showing supramolecular interactions.

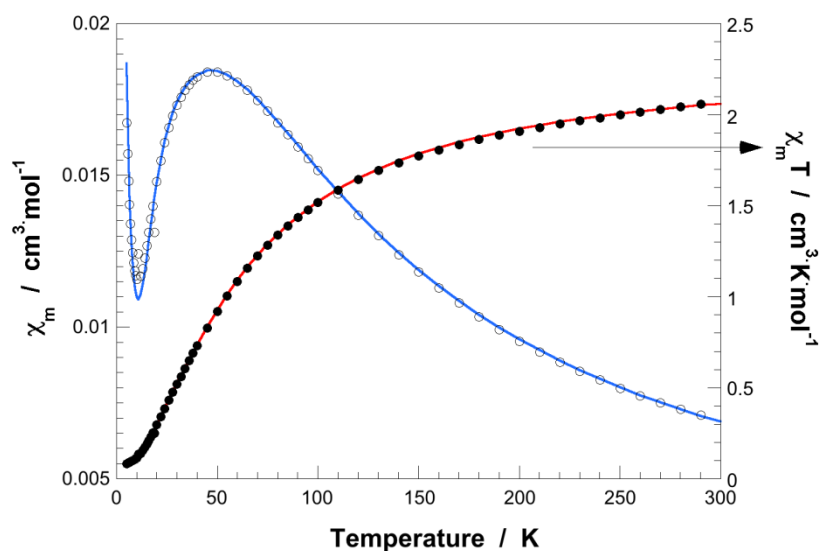


Figure S9. Thermal variation of χ_m and $\chi_m T$ for complex **1**. The solid lines correspond to the best fits obtained with Eq. 1.

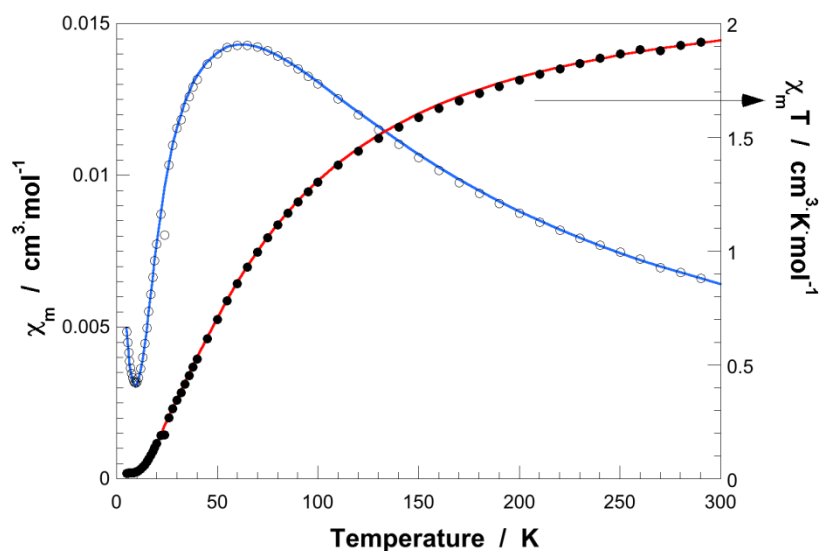


Figure S10. Thermal variation of χ_m and $\chi_m T$ for complex **2**. The solid lines correspond to the best fits obtained with Eq. 1.

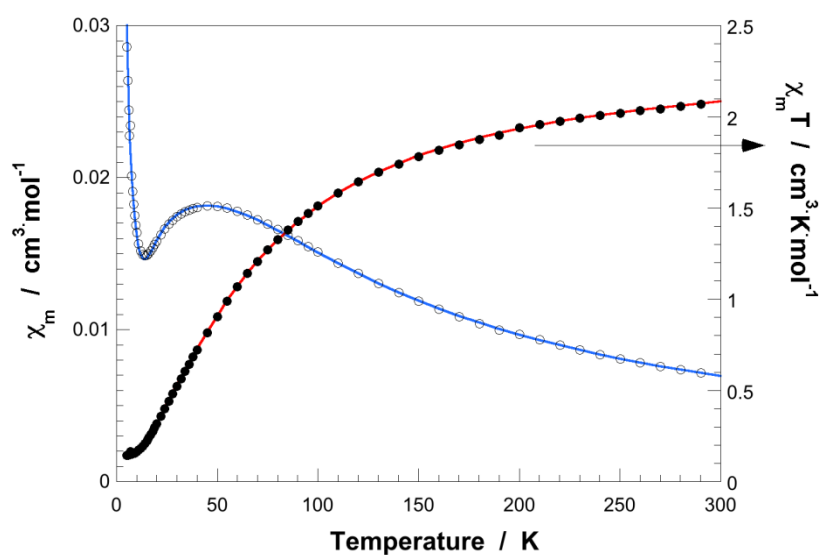


Figure S11. Thermal variation of χ_m and $\chi_m T$ for complex **4**. The solid lines correspond to the best fits obtained with Eq. 1.

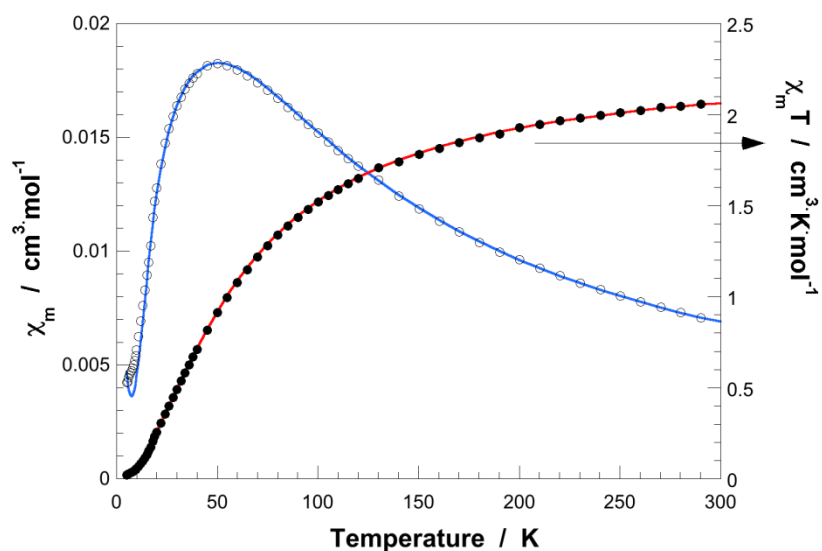


Figure S12. Thermal variation of χ_m and $\chi_m T$ for complex **5**. The solid lines correspond to the best fits obtained with Eq. 1.

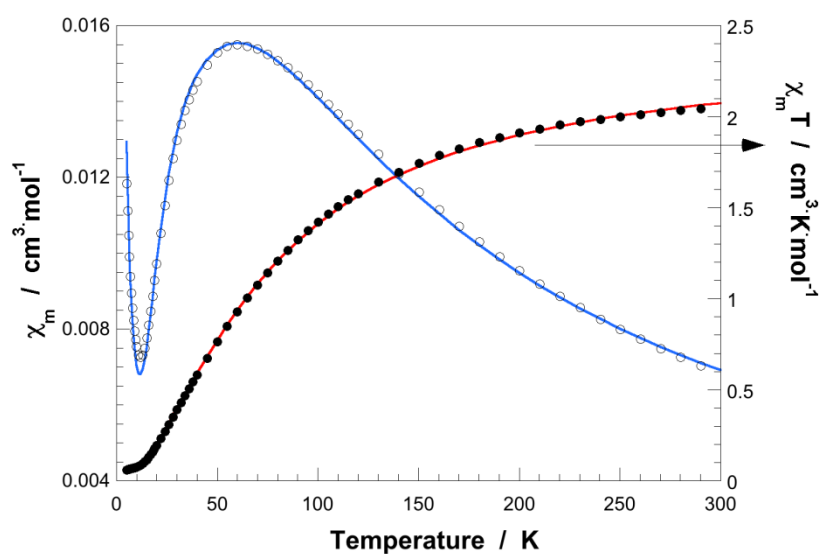


Figure S13. Thermal variation of χ_m and $\chi_m T$ for complex **6**. The solid lines correspond to the best fits obtained with Eq. 1.

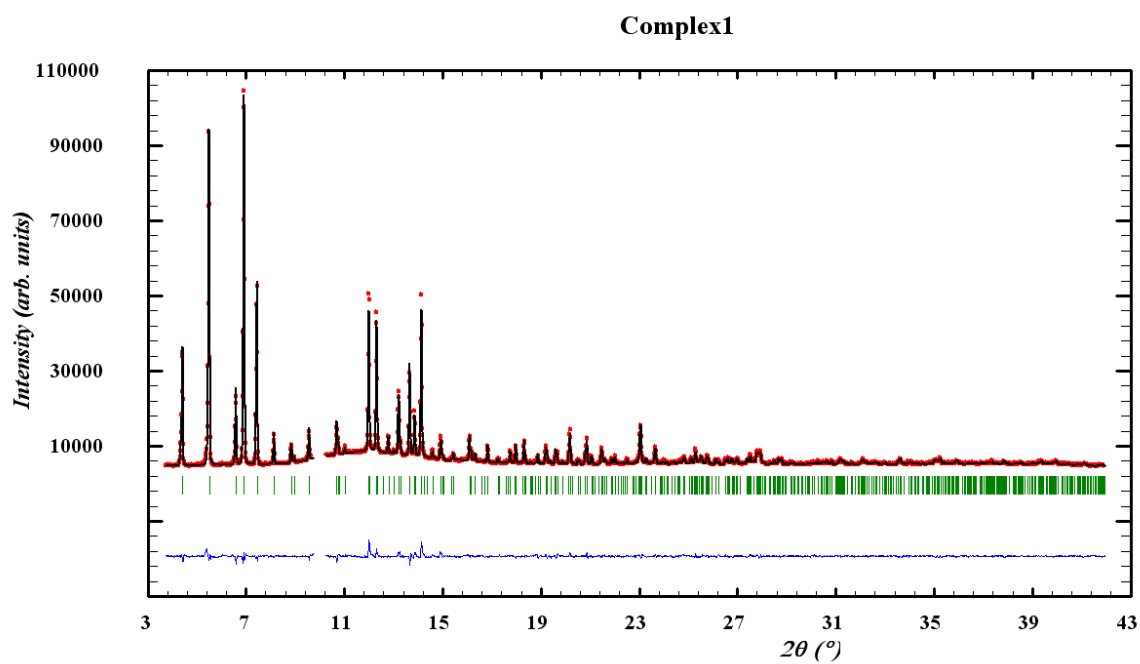


Figure S14: Plot for the Rietveld refinement of 1

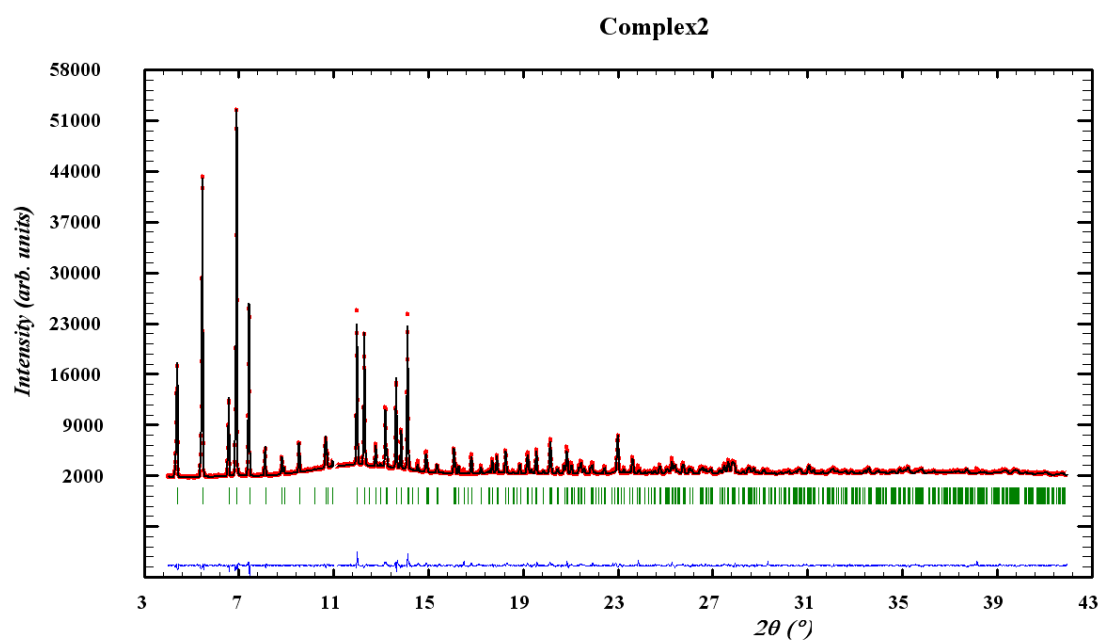


Figure S15: Plot for the Rietveld refinement of 2

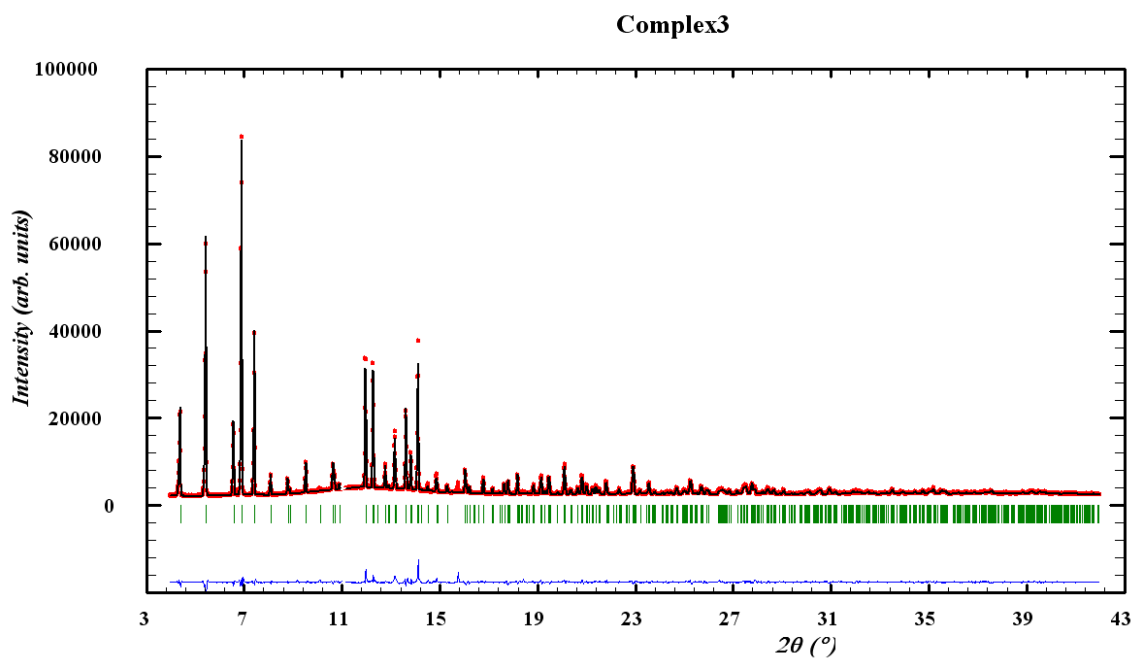


Figure S16: Plot for the Rietveld refinement of **3**